



**HAL**  
open science

# Exploiting optical flow field properties for 3D structure identification

Tan Khoa Mai, Michèle Gouiffes, Samia Bouchafa

► **To cite this version:**

Tan Khoa Mai, Michèle Gouiffes, Samia Bouchafa. Exploiting optical flow field properties for 3D structure identification. 14th International Conference on Informatics in Control, Automation and Robotics (ICINCO 2017), INSTICC, Jul 2017, Madrid, Spain. pp.459–464, 10.5220/0006474504590464 . hal-01609049

**HAL Id: hal-01609049**

**<https://hal.science/hal-01609049v1>**

Submitted on 9 Oct 2017

**HAL** is a multi-disciplinary open access archive for the deposit and dissemination of scientific research documents, whether they are published or not. The documents may come from teaching and research institutions in France or abroad, or from public or private research centers.

L'archive ouverte pluridisciplinaire **HAL**, est destinée au dépôt et à la diffusion de documents scientifiques de niveau recherche, publiés ou non, émanant des établissements d'enseignement et de recherche français ou étrangers, des laboratoires publics ou privés.

# Exploiting optical flow field properties for 3D structure identification

Tan Khoa Mai<sup>1</sup>, Michèle Gouiffès<sup>2</sup> and Samia Bouchafa<sup>1</sup>

<sup>1</sup> *IBISC, Univ. d'Evry Val d'Essonne, Université Paris Saclay*

<sup>2</sup> *LIMSI, CNRS, Univ. Paris Sud, Université Paris Saclay, F-91405 Orsay, France*  
*tan-khoa.mai, michele.gouiffes@limsi.fr, samia.bouchafa@ibisc.univ-evry.fr*

Keywords: Optical flow, c-velocity, 3-D plane reconstruction

Abstract: This paper deals with a new method that exploits optical flow field properties to simplify and strengthen the original c-velocity approach (Bouchafa and Zavidovique, 2012). C-velocity is a cumulative method based on a Hough-like transform adapted to velocities that allows 3D structure identification. In case of moving cameras, the 3D scene is assumed to be composed by a set of 3D planes that could be categorized in 3 main models : horizontal, lateral and vertical planes. We prove in this paper that, by using directly pixel coordinates to create what we will call the uv-velocity space, it is possible to detect 3D planes efficiently. We conduct our experiments on the KITTI optical flow dataset (Menze and Geiger, 2015) to prove our new concept besides the effectiveness of uv-velocity in detecting planes. In addition, we show how our approach could be applied to detect free navigation area (road), urban structures like buildings and obstacles from a moving camera in the context of Advanced Driver Assistance Systems.

## 1 INTRODUCTION

Advanced driver assistance systems are one of the fastest growing markets in the world<sup>1</sup> thanks to the constant development in security and intelligence of autonomous vehicles which has been the outcome of many works in this domain. For trajectory and obstacles detection tasks, ADAS systems are widely based on multi-sensors cooperation (Lidar, accelerometers, odometers, etc.) rather than on computer vision. However, data fusion from different sensors is not straightforward since sensors always provide imprecise and missing information. Moreover, most of these sensors are very specialized and provide limited information while vision can be used for many tasks like : scene structure analysis, motion analysis, recognition, and so on. Even if stereovision appears widely preferred in this context, it is very restrictive because of camera calibration or/and rectification step(s) (Lu et al., 2004). We propose to focus in our study on "monocular" vision for its several advantages including its cost, both economic and energetic, and the wealth of information extracted from monocular image sequences like (among others) obstacle motion.

Among all existing monocular approaches, we chose to focus on the c-velocity method (Bouchafa

and Zavidovique, 2012) because of its potential robustness. This method is based on the exhibition of constant velocity *loci* whose pattern is bound to the orientation of planes to be detected (e.g. horizontal or vertical). Velocities obtained from an optical flow technique are cumulated in the c-velocity space. Thanks to its cumulative nature, c-velocity has the advantage to be very robust toward optical flow imprecision. In the classical c-velocity approach, a voting space is designed for each plane category. Our study aims at detecting 3-D planes in image sequences by proposing a more efficient formulation of the original c-velocity approach. We consider the case where images are captured from a camera on-board a moving vehicle and deal with urban scenes. Unlike other 3-D reconstruction methods that require camera calibration (Lu et al., 2004), our method called "uv-velocity" offers, under few assumptions, a more generic way to reconstruct the 3D scene around the autonomous vehicle without any calibration. Many studies for ADAS applications deal with estimating egomotion of cameras (Luong and Faugeras, 1997, Azuma et al., 2010), detecting free navigable space (roads) or obstacles (Oliveira et al., 2016, Mohan, 2014), (Cai et al., 2016, Ren et al., 2017). The uv-velocity can do all of them without any learning algorithm.

In (Labayrade et al., 2002), the authors propose a method to detect the horizontal plane by using a

1. <https://www.mordorintelligence.com/industry-reports/advanced-driver-assistance-systems-market>

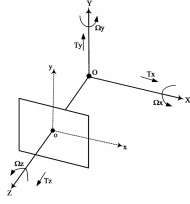


FIGURE 1: Coordinates system in case of a moving camera.

new histogram called the v-disparity map. Their work has inspired many works in lanes and obstacles detection for autonomous vehicles (Soquet et al., 2007, Qu et al., 2016). The c-velocity is the transposition of the v-disparity concept to motion : instead of stereo camera, c-velocity deals with monocular vision. The idea behind the c-velocity is that, under a pure translation of the camera, the norm  $\mathbf{w}$  of a velocity vector of a moving plane (estimated using an optical flow method) varies linearly with a pixel value that is called the *c-value* (or *c*). The latter is computed from only pixels position on the image plane. As in both the v-disparity method and in the classical Hough transform, 3D planes should be detected thanks to a line detection process in the c-velocity voting space. A re-projection is done to associate to each pair  $(c, \mathbf{w})$ , its corresponding set of pixels in the image. In the original c-velocity method, this process is not optimized since the estimation of two intermediate variables  $(c, \mathbf{w})$  is required and involve square root and power operations. However, in practice, obtained results from the c-velocity method confirms its reliability in real condition. Using the same methodology and assumptions than the c-velocity method, we find out that using only  $u$  or  $v$  components of the velocity vectors instead of the norm to create suitable voting spaces leads to more intuitive characteristics that make easier plane model interpretation. Moreover, we show that this new formulation can keep the performance of detections as well. The uv-velocity is more similar to the v-disparity than the c-velocity if we try to find an analogy. A tough problem like detecting horizontal 3D planes (resp. vertical planes) becomes - using the v-velocity (resp. u-velocity) - a simple parabola curve detection process in the defined voting space. Frontal planes (assimilated to obstacles in the 3D scene) can be detected in these two voting spaces by finding straight lines. After finding these curves in the voting space thanks to a Hough transform, we re-project the  $\mathbf{v}\cdot\mathbf{y}$  or  $\mathbf{u}\cdot\mathbf{x}$  back to the image to reveal planes. The paper is organized as follows : section 2 explains mathematically the chosen models and presents all required equations. Section 3 explains how to build the voting space and provides information about the curve detection process. Section 4 shows results of

our uv-velocity method for detecting 3D planes. Section 5 discusses the results and provides some ideas for future work.

## 2 MAIN ASSUMPTIONS AND MODELS

This section details the chosen camera coordinates system and gives the 2D projection of a 3-D plane motion. We assume that the 2D motion in the image could be approximated by the optical flow. We consider three relevant plane models in case of urban scenes : horizontal, lateral and vertical.

One can suppose an image sequence taken from a camera mounted on a moving vehicle. The optical axis of the camera is aligned with  $Z$  (see Fig.1).

Two frame coordinates are considered :  $OXYZ$  for representing 3-D points in real the 3D scene and  $oxy$  for representing the projection of these points on the image plane. A 3D point  $\mathbf{P}(X, Y, Z)$  is projected on the image plane at point  $\mathbf{p}(x, y)$  using the well-known projection equations :  $x = f \frac{X}{Z}$  and  $y = f \frac{Y}{Z}$ , where  $f$  is the focal length of the sensor.

In case of a moving camera, with a translational motion  $\mathbf{T} = [T_X, T_Y, T_Z]^T$  and a rotational motion  $\Omega = [\Omega_X, \Omega_Y, \Omega_Z]^T$ , according to (Bouchafa and Zavidovique, 2012), 2D motion vectors of pixels belonging to a 3D plane could be expressed as :

$$\begin{aligned} u &= \frac{xy}{f} \Omega_X - \left( \frac{x^2}{f} + f \right) \Omega_Y + y \Omega_Z + \frac{xT_Z - fT_X}{Z} \\ v &= -\frac{xy}{f} \Omega_Y + \left( \frac{y^2}{f} + f \right) \Omega_X + x \Omega_Z + \frac{yT_Z - fT_Y}{Z} \end{aligned} \quad (1)$$

2D motion vectors converge to a unique location in the image. This particular point, which depends on the translational motion, is called the Focus of Expansion (FOE) and its coordinates are given by :

$$x_{FOE} = \frac{f \times T_X}{T_Z} \text{ and } y_{FOE} = -\frac{f \times T_Y}{T_Z} \quad (2)$$

In case of a pure translational motion, (1) becomes :

$$u = \frac{xT_Z - fT_X}{Z} \text{ and } v = \frac{yT_Z - fT_Y}{Z} \quad (3)$$

A 3D plane is characterized by its distance  $d$  to the origin  $O$  and its normal vector  $\mathbf{n} = [n_X, n_Y, n_Z]^T$ , with equation :  $|n_X X + n_Y Y + n_Z Z| = d$ . All points visible by the camera have  $Z > 0$ . By dividing plane equation by  $Z$  and combining with projection equations, we get :

$$\frac{1}{fd} |n_X x + n_Y y + n_Z f| = \frac{1}{Z} \quad (4)$$

Replacing Z in Eq.3 by Z in Eq.4, 2D motion of a 3D plane is :

$$\begin{aligned} u &= \frac{1}{fd} |n_x x + n_y y + n_z f| (x T_Z - f T_X) \\ v &= \frac{1}{fd} |n_x x + n_y y + n_z f| (y T_Z - f T_Y) \end{aligned} \quad (5)$$

Since the translational motion  $\mathbf{T} = [T_X, T_Y, T_Z]^T$ , the focus  $f$  of the camera and the distance  $d$  are constant for a given plane, the Eq.5 represents the relation between the pixels coordinates and the 2D motion assimilated to the optical flow. Using this relation, planes can be easily detected without knowing neither the egomotion nor the intrinsic parameter  $f$  of the camera.

In urban scenes, without any loss of generality, three main plane models (horizontal, vertical, lateral) can be considered. They are characterized by their normal vectors :  $[0, 1, 0]^T$  for Horizontal planes,  $[0, 0, 1]^T$  for Vertical planes and  $[1, 0, 0]^T$  for Lateral planes. By injecting these normal vector values into Eq.5, the equation is declined into the three formulations given in Table.1. These equations reveal two terms : one of them depends only on pixel positions (it is called the c-value), the second one depends on the egomotion, the focal length and the plane-to-origin distance.

Planes	$u$	$v$
Horizontal	$\frac{T_Z}{fd_r}  y  (x - x_{FOE})$	$\frac{T_Z}{fd_r}  y  (y - y_{FOE})$
Vertical	$\frac{T_Z}{d_o} (x - x_{FOE})$	$\frac{T_Z}{d_o} (y - y_{FOE})$
Lateral	$\frac{T_Z}{fd_b}  x  (x - x_{FOE})$	$\frac{T_Z}{fd_b}  x  (y - y_{FOE})$

TABLE 1: 2D motion equations for three main plane models : horizontal, vertical and lateral.

In the original c-velocity method, the norm  $\mathbf{w} = \sqrt{u^2 + v^2}$  of a velocity vector and the c-value are used to create a 2D voting space where one of the axis is  $\mathbf{w}$  and the other is  $c$ . Since there is a linear relationship between them in case of moving planes, detecting lines in the c-velocity space is equivalent to detect 3D planes :

$$w = \frac{T_Z}{fd_r} y^2 \sqrt{(x - x_{FOE})^2 + (y - y_{FOE})^2} = K \times c \quad (6)$$

where  $c = y^2 \sqrt{(x - x_{FOE})^2 + (y - y_{FOE})^2}$ . Lines in the c-velocity space are detected using a classical Hough transform. In our case, we chose to consider separately the two components of a velocity vector. Each component could be exploited to detect a specific plane model. Let us study each of them separately in the following subsections.

## 2.1 Horizontal plane Model

In practice, in the context of ADAS, an horizontal plane represents the road on which the vehicle moves. For sake of simplicity, without compromising with reality, according to our model assumptions, road pixels are always located under the  $y_{FOE}$  in the image and the vertical position sign does not change for the whole road. From Table. 1, we have :

$$u = K_r y (x - x_{FOE}) \quad v = K_r y (y - y_{FOE}) \quad (7)$$

where  $K_r = \text{sign}(y) \frac{T_Z}{fd_r}$ . If  $|u|=\text{constant}$  (or  $|v|=\text{constant}$ ), from Eq.7, we can draw the iso-motion contours on the image. These contours show wherever the pixels have the same component  $u(v)$  if they belong to the road. In Fig.2(a,b), we set different values  $u$  and  $v$  and a constant  $K_r$  with  $x_{FOE} = y_{FOE} = 0$ . For the  $u$ -component, the image plane is divided into 4 symmetric quarters, each  $u$ -value creates a hyperbola which is a parallel to each others. Meanwhile for  $v$ -component, the image is divided into 2 symmetric halves by the line  $y_{FOE}$ , each  $v$ -value creates a straight line which is parallel to each other.

## 2.2 Lateral plane Model

From the vehicle, buildings can be considered as lateral planes. The principle is the same than for horizontal planes : iso-motion contours of a lateral plane are shown in Fig.2(c,d).

In this case, iso-motion contours of lateral planes are symmetric to those that could be computed for horizontal planes. The iso-motion contours of  $u$ -component forms a straight line parallel to the  $x_{FOE}$  line.

## 2.3 Vertical plane Model

Obstacles could be assimilated to vertical planes in front of vehicle. As we can see in the Fig.2(e,f), iso-motion contours of obstacle planes inherit the characteristics of both  $u$  component from lateral planes and  $v$  component from horizontal planes.

The straight line of iso-motion curve of  $v$ -component (horizontal plane) or  $u$ -component (lateral plane), that appears is an interesting characteristic that shows that it is possible to exploit  $u$  and  $v$  separately to build dedicated voting spaces.

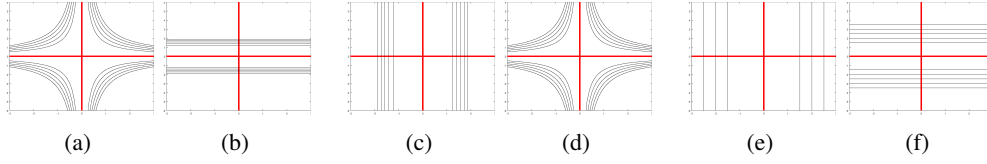


FIGURE 2: Iso-motion contours of  $u$ -component (a,c,e) and  $v$ -component (b,d,f) on the image for horizontal planes (a,b), lateral plane (c,d) and vertical plane (e,f). The red lines are the axes  $x$  (horizontal) and  $y$  (vertical). The origin is at their intersection.

### 3 UV-VELOCITY

In this section, we explain how to create  $uv$ -velocity voting spaces and how to exploit them to detect corresponding plane models.

#### 3.1 Voting spaces

Based on the analysis of iso-motion contours, we propose to detect three types of planes by using two voting spaces called  $u$ -velocity and  $v$ -velocity. Considering an image of size  $H \times W$ , these voting spaces are respectively of size  $W \times u_{max}$  and  $H \times v_{max}$ , where  $u_{max}$  and  $v_{max}$  are the maximum motion values.



FIGURE 3: The  $u$ -velocity before and after thresholding (top, bottom respectively) and the  $v$ -velocity before and after thresholding (left, right respectively) represent voting spaces corresponding to the optical field computed (middle) for an image sequence from the KITTI dataset.

Each row of the  $v$ -velocity space is a velocity histogram of the  $v$  components for each row in the image. In this space, the iso-motion contours for an horizontal plane form a parabola Fig.3(right) since:  $v = K_r y(y - y_{FOE}) = f(y)$  is a quadratic function which passes through the origin and  $y_{FOE}$ . From equations of Table.1, all pixels that belong to the vertical plane have the same  $v$ . It is the case also for each line but they form a straight line rather than a parabola Fig.4 (right). Moreover, for lateral planes,  $v$  varies with the change of  $x$ . They form arbitrary points with low intensity in the voting space which can be eliminated by using a threshold Fig.3(left to right, top to bottom), Fig.3 (left to right). Similarly, the  $u$ -velocity space Fig.3 (bottom) is a set of velocity histogram of the  $u$  components that are constructed by considering each

column of the motion image. The parabolas that appear on this voting space represent lateral planes. A straight line appears too if a vertical plane exists on the scene.



FIGURE 4: The  $v$ -velocity voting space before and after thresholding (left and right respectively) formed from the  $v$ -component of the image motion (middle). Using an optical flow ground truth, we can clearly see a parabola and a nearly straight line in the voting space.

#### 3.2 Analysis and interpretation

The previous subsection has shown how to construct suitable voting spaces for detecting each plane according to its model (horizontal/lateral/vertical). The next step consists in detecting lines and parabolas using a Hough transform, using a common strategy. In case of a translational motion  $T = [T_X, T_Y, T_Z]$ , considering a focus of expansion  $[x_{FOE}, y_{FOE}]$ , without loss of generality, and taking example of  $v$ -component of horizontal plane, we can do the following remarks.

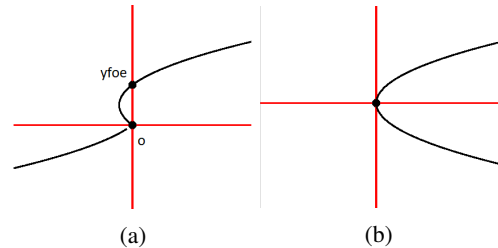


FIGURE 5: Illustration of one parabola finding on the voting space. Horizontal axes represent  $v$  (a) or  $|v|$  (b), with  $y_{FOE}$  and the origin is not interchangeable or is interchangeable respectively. The vertical axis represents the pixel's coordinates.

If we ignore  $v$  value sign, the parabola is unique for each horizontal plane but all parabolas share the same vertical-axes coordinates of vertex which is  $y_v = y_{FOE}/2$  but they have different horizontal-axes coordinates  $v = K_r|y_r|(y_r - y_{FOE})$  (see Fig.5(a)). In case of moving vehicles, the most important translation in terms of amplitude is toward the Z direction, that is  $T_X \approx 0$  and  $T_Y \approx 0$ , it means that  $x_{FOE} \approx 0$  and  $y_{FOE} \approx 0$ . So all parabolas share the same vertex point which is the origin (see Fig.5(b)). Consequently, all parabolas share the same form  $v = ay^2$  with  $a$  an unknown value. In order to detect parabolas, we propose a consensus voting process that leads to the estimation of parameter  $a$ .

Finally, the straight lines corresponding to the lateral planes are detected using the Hough transform after removing pixels that are already labeled as belonging to an horizontal or a vertical plane. For point of extension **FOE**, knowing that all translation motions will converge to or diverse from that point. A voting space where each optical flow draws a straight line on image are created where the point which has the most passages is the point of extension. Normally, this point does not deviate much from the center of image under our assumption.

## 4 EXPERIMENTS

To prove the validity of our approach, experiments are made using first the optical flow ground truth provided by KITTI and then with the optical flow estimation algorithm proposed by (Sun et al., 2010). For this first study, only the sequences where translational motion is dominant are considered. Figures 6 to 8 show a few examples, where the results of  $c$ -velocity and  $uv$ -velocity are put side by side for each kind of plane. All voting spaces are created using the absolute value of optical flow for  $uv$ -velocity. When using the optical flow ground truth (top), we got expected results : planes –especially the horizontal ones (see Fig. 6)– are correctly detected. Since the optical flow ground truth is not dense, we focus only on the vehicle and the road planes (Fig.6,8) since their attributes appear clearly on the voting space (Fig.4).

By using the optical flow computed from (Sun et al., 2010) (bottom of figures), the results are not as good as those we got with ground truth in terms of precision, occlusion handling (see Fig.6), but the voting spaces still reveal enough the expected curves like the one we see in Fig.3. When using the ground truth, the horizontal plane gives the most reliable results since it is always available on the image (it corresponds to the road). The detection of lateral planes

depends on the scene context, whether it has enough points to vote for a parabola. Using the Hough transform, the obstacle plane seems to be unstable, since, for instance, a car always contains many planes. It means that we have to consider voting space cooperation as future work. However, for some scenes, when the line appears clearly like in Fig.8, the obstacle can be detected correctly.

As we can see on Fig.6,7, the  $uv$ -velocity give almost the same performance as  $c$ -velocity whatever the optical flow, but it avoids expensive calculations like square-root or exponential and intermediate value  $c$ .

## 5 CONCLUSION

This paper has shown how to detect 3D planes in a Manhattan world using a specific voting space called  $uv$ -velocity. Its construction is based on the exploitation of optical flow intrinsic properties of moving planes and more particularly on iso-velocity curves. Results on ground-truth optical flows prove the efficiency of our new concept, when planes have enough pixels on the image to be detected. Experiments show that the precision of the results depends on the the quality of the input optical flow. In theory, the interference of other plane models on voting spaces will not cause much side effects on curve detection because there contribution in the voting space is low and could be eliminated by a simple threshold. In practice, we show that these interferences can complicate line and parabola detection. One of our futures works is then to propose a cooperation strategy between voting spaces. Moreover, since the quality of optical flow is directly related to the spread of the line or the parabolas in the voting space, it is possible to find a metric to find the parabola and refine the optical flow at the same time (Mai et al., 2017). Finally, rotational motion will be investigated in next steps to make the results more general.

## REFERENCES

- Azuma, T., Sugimoto, S., and Okutomi, M. (2010). Egomotion estimation using planar and non-planar constraints. In *2010 IEEE Intelligent Vehicles Symposium*, pages 855–862.
- Bouchafa, S. and Zavidovique, B. (2012).  $c$ -Velocity : A Flow-Cumulating Uncalibrated Approach for 3d Plane Detection. *International Journal of Computer Vision*, 97(2) :148–166.
- Cai, Z., Fan, Q., Feris, R. S., and Vasconcelos, N. (2016). A Unified Multi-scale Deep Convolutional Neural Net-



FIGURE 6: Horizontal plane detection based on the c-velocity voting space (a) and v-velocity voting space (b) using the optical flow ground truth (top) and an estimated optical flow (bottom)



FIGURE 7: Lateral planes detection whenever they are available on image based on the c-velocity voting space (a) and v-velocity voting space (b) using the estimated optical flow



FIGURE 8: Obstacle detection based on the v-velocity voting space using the optical flow ground truth

- work for Fast Object Detection. In *Computer Vision – ECCV 2016*, pages 354–370. Springer, Cham.
- Labayrade, R., Aubert, D., and Tarel, J. P. (2002). Real time obstacle detection in stereovision on non flat road geometry through "v-disparity" representation. In *IEEE Intelligent Vehicle Symposium, 2002*, volume 2, pages 646–651 vol.2.
- Lu, Y., Zhang, J. Z., Wu, Q. M. J., and Li, Z.-N. (2004). A survey of motion-parallax-based 3-D reconstruction algorithms. *IEEE Transactions on Systems, Man, and Cybernetics, Part C (Applications and Reviews)*, 34(4) :532–548.
- Luong, Q.-T. and Faugeras, O. D. (1997). Camera Calibration, Scene Motion and Structure recovery from point correspondences and fundamental matrices. *Ijcv*, 22 :261–289.
- Mai, T. K., Gouiffes, M., and Bouchafa, S. (2017). Optical flow refinement using reliable flow propagation. In *Proceedings of the 12th International Joint Conference on Computer Vision, Imaging and Computer Graphics Theory and Applications - Volume 6 : VISAPP, (VISIGRAPP 2017)*, pages 451–458.
- Menze, M. and Geiger, A. (2015). Object scene flow for autonomous vehicles. In *Conference on Computer Vision and Pattern Recognition (CVPR)*.
- Mohan, R. (2014). Deep deconvolutional networks for scene parsing.
- Oliveira, G. L., Burgard, W., and Brox, T. (2016). Efficient Deep Models for Monocular Road Segmentation.
- Qu, L., Wang, K., Chen, L., Gu, Y., and Zhang, X. (2016). Free Space Estimation on Nonflat Plane Based on V-Disparity. *IEEE Signal Processing Letters*, 23(11) :1617–1621.
- Ren, J., Chen, X., Liu, J., Sun, W., Pang, J., Yan, Q., Tai, Y.-W., and Xu, L. (2017). Accurate Single Stage Detector Using Recurrent Rolling Convolution. *arXiv :1704.05776 [cs]*. arXiv : 1704.05776.
- Soquet, N., Aubert, D., and Hautiere, N. (2007). Road Segmentation Supervised by an Extended V-Disparity Algorithm for Autonomous Navigation. In *2007 IEEE Intelligent Vehicles Symposium*, pages 160–165.
- Sun, D., Roth, S., and Black, M. J. (2010). Secrets of optical flow estimation and their principles. pages 2432–2439. IEEE.